Proceedings of the 32nd European Safety and Reliability Conference (ESREL 2022)
Edited by Maria Chiara Leva, Edoardo Patelli, Luca Podofillini, and Simon Wilson
 Published by Research Publishing, Singapore.
doi: 10.3850/978-981-18-5183-4_R01-04-288-cd

Designing reliable, data-driven maintenance for aircraft systems with applications to the aircraft landing gear brakes

Juseong Lee

Faculty of Aerospace Engineering, Delft University of Technology, The Netherlands
E-mail: J.Lee-2@tudelft.nl

Mihaela Mitici

Faculty of Aerospace Engineering, Delft University of Technology, The Netherlands
E-mail: M.A.Mitici@tudelft.nl

Sunyue Geng

Faculty of Technology, Policy, and Management, Delft University of Technology, The Netherlands
E-mail: s.geng@tudelft.nl

Ming Yang

Faculty of Technology, Policy, and Management, Delft University of Technology, The Netherlands
E-mail: m.yang-1@tudelft.nl

When designing the maintenance of multi-component aircraft systems, we consider parameters such as safety margins (used when component replacements are scheduled), and reliability thresholds (used to define data-driven Remaining-Useful-Life prognostics of components). We propose Gaussian process learning and novel adaptive sampling techniques to efficiently optimize these design parameters. We illustrate our approach for aircraft landing gear bakes. Data-driven, Remaining-Useful-Life prognostics for brakes are obtained using a Bayesian linear regression. Pareto optimal safety margins for scheduling brake replacements are identified, together with Pareto optimal reliability thresholds for prognostics.

Keywords: aircraft maintenance, predictive maintenance, data-driven maintenance, Remaining-Useful-Life prognostics, Gaussian process, design space exploration.

1. Introduction

The increasing use of condition-monitoring sensors of aircraft has generated a paradigm shift to data-driven, predictive maintenance: on-board sensors continuously monitor the degradation of components, Remaining-Useful-Life (RUL) prognostics are predicted using the sensor data, and components are replaced based on these RULs. When performing predictive maintenance, safety margins are used to schedule maintenance tasks. For example, a safety margin of μ days may be used to schedule a component replacement μ days *earlier* than the estimated RUL of the component. Also, the RUL prognostics themselves are defined based on reliability thresholds. For example, the RUL of a component is defined such that the probability of a severe degradation is smaller than a reliability threshold ξ ($0 < \xi < 1$). We are interested in specifying such maintenance design parameters (e.g., safety margins and reliability thresholds) that maximize the mean-cycle-to-replacement of components while minimizing the number of maintenance-related incidents due to unexpectedly high degradation levels.

Several studies integrate data-driven RUL prognostics into maintenance planning of different systems. In Arismendi et al. (2019), a framework for degradation prognostics and maintenance planning for bridges is proposed using a Markov decision process. In de Pater et al. (2022), the authors obtain RUL prognostics for aircraft turbofan engines using a Convolutional Neural Network and use the prognostics to trigger alarms and maintenance tasks. In de Pater and Mitici (2021), a

generic reliability threshold for RUL prognostics is used when planning maintenance for aircraft components. In general, however, a framework to identify optimal values for safety margins and reliability thresholds used when planning maintenance, is lacking. Often, these design parameters are selected by testing all possible values (brute-force) approach, which is inefficient.

In this paper, we propose a Gaussian process learning algorithm with adaptive sampling to efficiently optimize maintenance design parameters (safety margins used to schedule component replacements, reliability thresholds for RUL prognostics) such that the mean-cycle-to-replacement of components is maximized and the number of degradation-related incidents is minimized. We illustrate our algorithm for the maintenance of aircraft landing gear brakes. For the aircraft maintenance problem, we consider a stochastic degradation of the brakes based on actual data obtained from a fleet of aircraft. We also develop RUL prognostics for the brakes using a Bayesian linear regression. Finally, we efficiently obtain multiple combinations of values for the schedule-related safety margin and prognostics-related reliability thresholds, which leads to a Pareto front of the maintenance process of the aircraft brakes.

2. Predictive Maintenance for Aircraft

Aircraft is operated based on a sequence of flight cycles. Flight cycle i is defined by a departure time (τ_i^{dep}) and an arrival time (τ_i^{arr}). The time between the departure and arrival ($t \in [\tau_i^{\text{dep}}, \tau_i^{\text{arr}}]$) is called the *flight-time*. The time between the arrival and the next departure ($t \in [\tau_i^{\text{arr}}, \tau_{i+1}^{\text{dep}}]$) is called the *ground-time*, when maintenance can be performed.

2.1. *Degradation of landing gear brakes*

We consider the maintenance of aircraft landing gear brakes. A main part of a brake is the carbon disk. Over time, its thickness decreases due to erosion. The reduced thickness of the carbon disk is a direct indicator of the degradation of a brake. Lee and Mitici (2020) Let the degradation of the carbon disk of a brake follow a stochastic Gamma process $Z(t)$. The degradation of the brake during flight cycle i is:

$$Z(\tau_i^{\text{arr}}) - Z(\tau_i^{\text{dep}}) \sim \text{Gamma}(\alpha, \beta) \qquad (1)$$

where α is the shape parameter and β is the scale parameter of the Gamma process.

During the ground-time, if no maintenance is performed, the degradation level remains the same since the brakes are not used, i.e.,

$$Z(\tau_{i+1}^{\text{dep}}) - Z(\tau_i^{\text{arr}}) = 0. \qquad (2)$$

If a brake is replaced during the ground time before flight cycle i, $Z(\tau_i^{\text{dep}}) = 0$.

As soon as the degradation level exceeds a threshold η, we say that the brake is *inoperable*. The threshold η is specified by the manufacturer of the brakes, and reflects the mechanical properties of the brakes. After a proper normalization, we consider $\eta = 1$.

2.2. *Redundancy of the Landing Gear System and Degradation Incidents*

We say that a multi-component system has ${}_N\text{C}_M$ redundancy if the system consists of N components and needs to have at least M *operable* components, $(0 < M \leq N)$. As soon as more than $(N - M)$ components become inoperable, we say that a *degradation incident* occurs.

The aircraft landing gear system has 8 brakes in total, with 4 brakes on each side of the aircraft. At least 3 brakes on each side of the aircraft are required to be operational Lee and Mitici (2022), i.e., ${}_4\text{C}_3$ redundancy for each group of 4 brakes. As soon as more than one brake becomes inoperable on either side of the aircraft we say that we have a *degradation incident*.

2.3. *Condition monitoring*

Sensors continuously monitor the degradation level of the brakes. Let $\tilde{Z}_i$ be the degradation level indicated by the sensors after flight cycle i,

$$\tilde{Z}_i = Z_i + \epsilon_s, \qquad (3)$$

with $\epsilon_s \sim \mathcal{N}(0, \sigma_s^2)$ is the sensor measurement error.

2.4. *RUL prognostics for aircraft brakes*

We analyze the degradation of landing gear brakes recorded by sensors for a fleet of aircraft. Since the observed degradation exhibit a linear trend (see Fig.1), we use a Bayesian linear regression (BLR) to predict the Remaining-Useful-Life (RUL) of the brakes. Oikonomou et al. (2022)

The input of the BLR model is the degradation of the brake observed up to current flight cycle i_1, $\mathcal{Z} = \{(i, \tilde{Z}_i)|i_0 \leq i \leq i_1\}$, with an initial degradation level $\tilde{Z}_{i_0}$. We estimate the degradation level after flight cycle i as:

$$\tilde{Z}_i \sim \mathcal{N}(w_0 + w_1 i, \sigma^2_{BLR}) \tag{4}$$

where ω_0 is the intercept, ω_1 is the coefficient of the linear model, and σ^2_{BLR} is the variance of the Gaussian model. The prior of the coefficient ω_1 is assumed to be zero-mean Gaussian, i.e., $P(\omega_1) = \mathcal{N}(\omega_1|0, \lambda\mathbf{I})$. Here, λ and σ^2 are the hyper-parameters of the model, and we consider a Gamma distribution as their prior. Finally, the parameters ω_1, λ, and σ^2 are jointly optimized by maximizing the log marginal likelihood. The intercept ω_0 is the mean bias of the model in the input data $\mathcal{Z}$, i.e., $\omega_0 = \sum_{(i,\tilde{Z}_i)\in\mathcal{Z}}[\tilde{Z}_i - w_1 i]/|\mathcal{Z}|$.

Given that a brake has already been used for i flight cycles, its RUL $\rho(i)$ is the number of remaining flight cycles until the probability that the degradation level exceeds η, is larger than a reliability threshold ξ, i.e.,

$$\rho(i) = \min_{\delta}\left\{\delta \,:\, P\left(\tilde{Z}_{i+\delta} \geq \eta|\mathcal{Z}\right) \geq \xi\right\}. \tag{5}$$

The RUL prognostics $\rho(i)$ of the brakes are updated after every flight cycle, taking into account the most recently available degradation data $\mathcal{Z}$ collected from the on-board sensors.

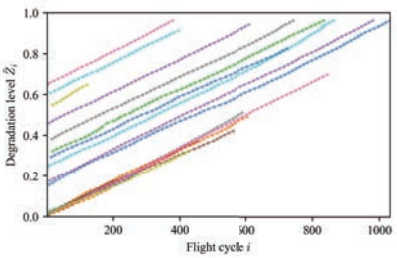

Fig. 1. Examples of degradation of the carbon disk of landing gear brakes.

2.5. *Maintenance using data-driven Remaining-Useful-Life prognostics*

We propose a predictive maintenance strategy that schedules brake replacements based on RUL prognostics. Specifically, a brake replacement is scheduled after $\left(\rho(i) - \mu\right)$ flight cycles, where $\rho(i)$ is the RUL prognostics of the brake obtained after the brake has been used for i flight cycles, and μ is a safety margin. So, we schedule a brake replacement μ flight cycles *earlier* than the estimated RUL $\rho(i)$.

Our predictive maintenance strategy has two design parameters to be optimized: i) the safety margin μ based on which a replacement is scheduled, and ii) the reliability threshold ξ used when determining the RUL $\rho(i)$. These two design parameters are selected from the continuous ranges $\mu \in [\mu_{\min}, \mu_{\max}]$ and $\xi \in [\xi_{\min}, \xi_{\max}]$.

The goal is to efficiently search in the continuous design space $[\mu_{\min}, \mu_{\max}] \times [\xi_{\min}, \xi_{\max}]$ for those values ξ and μ that optimize the maintenance with respect to multiple objectives.

2.6. *Objectives of Predictive Maintenance*

When designing the maintenance of aircraft, multiple (conflicting) objectives should be considered such as reliability-related objectives, cost-related objectives, efficiency-related objectives. We consider the following two objectives f_1 and f_2. Lee and Mitici (2021)

f_1 : Mean flight cycles to replace (MCTR),
f_2 : The expected number of degradation incidents (N_{Inc}) (see Section 2.2).

A large MCTR indicates that the mean time between two consecutive replacements of a brake is large, i.e., we utilize brakes efficiently. A low N_{Inc} implies that a limited number of degradation incidents are expected, i.e., the maintenance is reliable. The goal is to find optimal values for μ and ξ that maximize f_1 : MCTR and minimize $f_2 : N_{\text{Inc}}$.

For each combination of values for μ and ξ, Monte Carlo simulation is used to evaluate

MCTR and N_{Inc}. However, evaluating a large number of combinations of values for μ and ξ is computationally inefficient. Moreover, since the design space ($[\mu_{\min}, \mu_{\max}] \times [\xi_{\min}, \xi_{\max}]$) is continuous, it is not possible to evaluate all possible values anyways. Therefore, we are interested in using a minimum number of simulations to efficiently determine Pareto optimal values of μ and ξ.

3. Efficiently Exploring the Design Space of the Maintenance Problem

We pose the design of the maintenance of the landing gear brakes as a design space exploration problem, i.e., we are identifying the design vectors $\mathbf{x} = [\mu, \xi]$ that optimize multiple objectives $\mathbf{f}(\mathbf{x}) = [\mathrm{MCTR}, N_{\mathrm{Inc}}]$ by exploring the design space $\mathcal{X} = [\mu_{\min}, \mu_{\max}] \times [\xi_{\min}, \xi_{\max}]$.

We propose Gaussian process (GP) learning with adaptive sampling to efficiently explore the design space $\mathcal{X}$.

Evaluate the objectives and update the Pareto front

At each iteration k, we evaluate the objectives $\mathbf{f}(\mathbf{x})$ of sampled parameter values $\mathbf{x} \in \mathcal{X}_k \subset \mathcal{X}$. At the initial iteration $k = 0$, we sample $\mathbf{x} \in \mathcal{X}_0$ using an l-level factorial design method. Kleijnen (2008) This evaluation is made by Monte Carlo simulation of the aircraft maintenance process given in Section 2.

Given the Monte Carlo simulation results, we identify the set of Pareto optimal parameters $\mathcal{X}_k^*$:

$$\mathcal{X}_k^* = \{\mathbf{x} \mid \nexists \mathbf{x}' : \mathbf{f}(\mathbf{x}') \succ \mathbf{f}(\mathbf{x}), \forall \mathbf{x}' \in \bigcup_{0,\dots,k} \mathcal{X}_k\}. \tag{6}$$

Here, $\mathbf{f}(\mathbf{x}') \succ \mathbf{f}(\mathbf{x})$ implies that $\mathbf{f}(\mathbf{x}')$ dominates $\mathbf{f}(\mathbf{x})$ according to the Pareto efficiency. As such, $\mathcal{X}_k^*$ is an approximation of the true Pareto front $\mathcal{X}^*$ because $\bigcup_{0,\dots,k} \mathcal{X}_k \subset \mathcal{X}$.

We propose to refine $\mathcal{X}_k^*$ by exploring and evaluating new $\mathbf{x}$ that is expected to be Pareto optimal using GP learning models.

Train Gaussian Process learning models

We construct GP learning models to rapidly pre-estimate $\mathbf{f}(\mathbf{x})$ without using Monte Carlo simulations. Let $g_m(\mathbf{x})$ be a GP model mapping $\mathbf{x}$ into an objective f_m. A GP model is defined by a mean function and a covariance function. Rasmussen and Williams (2006) Assuming a zero prior mean function, g_m is defined as:

$$g_m(\mathbf{x}) = \mathcal{GP}\Big(0, \kappa_m(\mathbf{x}, \mathbf{x}')\Big), \tag{7}$$

where κ_m is a covariance function, or equivalently a *kernel*. For simplicity, we drop the the subscript m in the following discussion about kernels. We select the following compound kernel function:

$$\kappa(\mathbf{x}, \mathbf{x}') = \kappa_{\mathrm{RBF}}(\mathbf{x}, \mathbf{x}') + \kappa_{\mathrm{WN}}(\mathbf{x}, \mathbf{x}'), \tag{8}$$

where κ_{RBF} is a squared exponential radial basis function (RBF) kernel, and κ_{WN} is a white noise (WN) kernel.

The RBF kernel κ_{RBF} is defined based on an Euclidean distance as follows:

$$\kappa_{\mathrm{RBF}}(\mathbf{x}, \mathbf{x}') = \exp\left(-\frac{1}{2}\sum_{n=1}^{N}\left(\frac{x_n - x_n'}{l_n}\right)^2\right), \tag{9}$$

where x_n is n^{th} element of vector $\mathbf{x}$, and l_n is a characteristic length-scale. Depending on l_i, the intensities of the correlation along design parameter x_n varies.

The WN kernel κ_{WN} models the homogeneous noise in the objective values in the training data. Rojas-Gonzalez and Van Nieuwenhuyse (2020) The WN kernel κ_{WN} is defined as follows:

$$\kappa_{\mathrm{WN}}(\mathbf{x}, \mathbf{x}') = \begin{cases} \sigma^2_{\mathrm{noise}}, & \text{if } \mathbf{x} = \mathbf{x}' \\ 0, & \text{otherwise,} \end{cases} \tag{10}$$

where $\sigma^2_{\mathrm{noise}} > 0$ is a noise level.

Given this compound kernel, we train the GP models $g_m(x)$ in Eq.(7). The training data $\mathcal{D}_k$ is the Monte Carlo simulation results obtained until the current iteration k, i.e., $\mathcal{D}_k = \{(\mathbf{x}, \mathbf{f}(\mathbf{x})) \mid \mathbf{x} \in \bigcup_{0,\dots,k} \mathcal{X}_k\}$. The hyper-parameters l_i in Eq.(9) and $\sigma^2_{\mathrm{noise}}$ in Eq.(10) are optimized using the maximum likelihood estimation. The trained GP models are used to rapidly pre-estimate the objective vectors during the following adaptive sampling step.

Adaptive sampling

Now we select $\mathbf{x}$ for the next iteration $(k+1)$ using adaptive sampling to balance exploration and

exploitation. Here, *exploration* implies acquiring training data and improving the GP models, and *exploitation* means improving the current solution ($\mathcal{X}_k^*$). Chen et al. (2009) The adaptive sampling has two steps, we first sample $\mathbf{x} \in \mathcal{X}$ based on global sampling and local sampling. Global sampling enables to explore the unknown domain space, while local sampling allows to exploit the current Pareto optimal solutions to generate additional x. Then, among the sampled $\mathbf{x}$, we select the promising ones based on their objective vectors pre-estimated by the GP models. This adaptive sampling approach reduces the number of $\mathbf{x}$ to simulate, and balances the ratio of the exploration to the exploitation.

For global sampling, $\mathbf{x}$ is sampled independently of the training data obtained so far (exploration). Local sampling is based on the idea that Pareto optimal $\mathbf{x}$ is likely to be located in the vicinity of the other Pareto optimal parameter values (exploitation). We sample $\mathbf{x}$ from a convex combinations of two Pareto optimal solutions $\mathbf{x}_1, \mathbf{x}_2 \in \mathcal{X}_k^*$, i.e.,

$$\mathbf{x} = w\mathbf{x}_1 + (1-w)\mathbf{x}_2, \tag{11}$$

with $0 < w < 1$.

For all sampled $\mathbf{x}$, we pre-estimate their objective vectors $\hat{\mathbf{f}}(\mathbf{x}) = [\hat{f}_1(\mathbf{x}), \hat{f}_2(\mathbf{x})]$. Here $\hat{f}_m(\mathbf{x})$ is the prediction made by the GP model g_m, whose posterior distribution is normally distributed when the training data $\mathcal{D}_k$ is given Rasmussen and Williams (2006), i.e.,

$$f_m(\mathbf{x})|\mathbf{x}, \mathcal{D}_k \sim \mathcal{N}(\mathbb{E}[f_m], \mathbb{V}[f_m]). \tag{12}$$

Here, the mean $\mathbb{E}[f_m]$ and variance $\mathbb{V}[f_m]$ are:

$$\mathbb{E}[f_m] = K(\mathbf{x}, X_k)\big[K(X,X)\big]^{-1} F_m, \tag{13}$$

$$\begin{aligned}\mathbb{V}[f_m] &= K(\mathbf{x},\mathbf{x}) \\ &- K(\mathbf{x}, X_k)\big[K(X_k, X_k)\big]^{-1} K(X_k, \mathbf{x}),\end{aligned} \tag{14}$$

where X_k is the matrix of $\mathbf{x}$ in $\mathcal{D}_k$, F_m^s is the vector of f_m in $\mathcal{D}_k$, $K(\cdot,\cdot)$ is the covariance matrix calculated by the kernel $\kappa(\cdot,\cdot)$ in Eq.(8).

This posterior distribution in Eq.(12) of the GP model gives both the prediction $\mathbb{E}[f_m]$, and its uncertainty $\mathbb{V}[f_m]$. Assuming that f_m is minimized, we estimate $\hat{f}_m(x)$ as the lower confidence

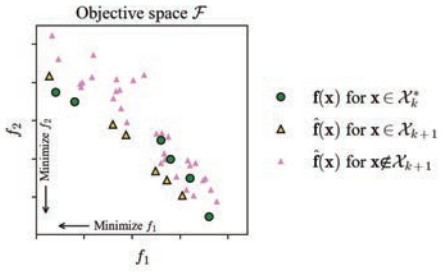

Fig. 2. Adaptive sampling in the objective space $\mathcal{F}$.

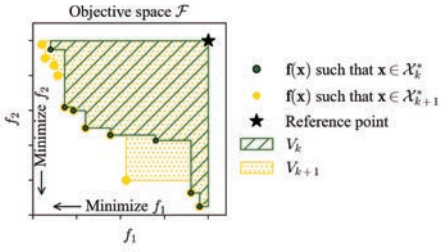

Fig. 3. A visualization of hyper-volume indicator V at iteration k and $(k+1)$.

interval of Eq.(12), i.e.,

$$\hat{f}_m(x) = \mathbb{E}[f_m] - \zeta\sqrt{\mathbb{V}[f_m]}, \tag{15}$$

where $\zeta \geq 0$ is a constant determining the width of the confidence interval.

Finally, we select $\mathbf{x}$ whose $\hat{\mathbf{f}}(\mathbf{x})$ is non-dominated. Let $\mathcal{X}_{k+1}$ be a set of $\mathbf{x}$ selected for the next iteration $(k+1)$. Then, we start the next iteration $(k+1)$ by evaluating the objectives of $\mathbf{x} \in \mathcal{X}_{k+1}$.

Fig. 2 shows an example of an adaptive sampling step in the objective space $\mathcal{F}$, $\mathbf{f} \in \mathcal{F}$. Circles represent the Pareto optimal objective vectors obtained up to iteration k. Triangles represent the objective vectors $\hat{\mathbf{f}}(\mathbf{x})$ pre-estimated by the GP models. We only select $\mathbf{x}$ if $\hat{\mathbf{f}}(\mathbf{x})$ is non-dominated. Yellow triangles are associated with $\mathbf{x}$ selected for the next iteration because $\hat{\mathbf{f}}(\mathbf{x})$ are non-dominated, while pink triangles are not selected.

Stopping criteria and quality indicators

We stop the iterations if a predefined number of Monte Carlo simulations is exceeded. Then, we

assess whether the quality of the identified Pareto front is satisfactory/saturated, by evaluating two indicators. One is the number of Pareto optimal parameter values $\mathbf{x}$ obtained during k iterations, i.e., $|\mathcal{X}_k^*|$. The other is a hyper-volume indicator V_k obtained based on the obtained Pareto front after iteration k. V_k is the hyper-volume in the objective space $\mathcal{F}$, covered by a reference point and the Pareto front. Zitzler et al. (2003)

Fig. 3 visualizes the hyper-volume indicators V_k and V_{k+1} for a 2 dimensional objective space $\mathcal{F}$, where f_1 and f_2 are minimized. The green and yellow circles denote the Pareto optimal objective vectors obtained during iteration k and $(k+1)$, respectively. The star at the upper right corner is the reference point that covers the hyper-volumes.

4. Case study: Predictive Maintenance of Aircraft Landing Gear Systems

We consider 2 aircraft landing gear systems, one on each side of the wing. Each landing gear system has 4 brakes with ${}_4\mathrm{C}_3$ redundancy. The degradation of the brakes are assumed to follow a Gamma process with parameters $\alpha = 0.8$ and $\beta = 0.001$. Sensors monitor the degradation of the brakes. The measurement error of the sensors is assumed to be normally distributed with mean zero and $\sigma_s = 0.0204$. Lee and Mitici (2020)

The design space $\mathcal{X}$ is defined by the range of the two design parameters μ (safety margin used when scheduling maintenance) and ξ (reliability threshold used to determine RUL). We explore the following ranges:

$$\begin{aligned}\mu \in&[\mu_{\min}, \mu_{\max}] = [0, 30],\\ \xi \in&[\xi_{\min}, \xi_{\max}] = [0.01, 0.99].\end{aligned}$$

Fig. 4 shows the exploration of the design space during iterations $k = 1, 2, 3$. Here, the Pareto optimal parameter values $\mathbf{x} \in \mathcal{X}_k^*$ are marked with green squares in the design space, and their objective vectors $\mathbf{f}(\mathbf{x})$ are marked with green circles in the objective space. At iteration $k = 1$, we conducted Monte Carlo simulations of 12 parameter values $\mathbf{x} \in \mathcal{X}_1$, i.e., $|\mathcal{X}_1| = 12$. Among them, seven parameter values were identified as Pareto optimal solutions, i.e., $|\mathcal{X}_1^*| = 7$.

Next, we trained the GP models using the training data obtained by the Monte Carlo simulation, i.e., $\{(\mathbf{x}, \mathbf{f}(\mathbf{x})) \mid \mathbf{x} \in \mathcal{X}_1\}$. Based on the adaptive sampling approach, we selected five new design parameters $\mathbf{x}$ to be simulated in the next iteration $k = 2$, i.e, $|\mathcal{X}_2| = 5$. These $\mathbf{x} \in \mathcal{X}_2$ are marked with yellow diamonds in the design space ($k = 1$), and their objective vectors $\hat{\mathbf{f}}(\mathbf{x})$ predicted by the GP models are marked as yellow triangles in the objective space ($k = 1$). For example, see $\mathbf{x}_1, \mathbf{x}_2 \in \mathcal{X}_2$ in the design space ($k = 1$) in Fig. 4.

At iteration $k = 2$, we conducted Monte Carlo simulations for the selected parameter values $\mathbf{x} \in \mathcal{X}_2$. Given their objective vectors assessed by Monte Carlo simulation, we updated the Pareto optimal solutions $\mathcal{X}_2^*$. For instance, $\mathbf{x}_2$ was identified as Pareto optimal solution and was included to $\mathcal{X}_2^*$. On the other hand, $\mathbf{x}_1$ was dominated by solutions already obtained at iteration $k = 1$, and thus it was excluded from $\mathcal{X}_2^*$. We repeated these steps until iteration $k = 19$.

4.1. *Pareto optimal maintenance*

The final design for the maintenance of the aircraft brakes is shown in Fig.5. We have simulated 102 parameters during 19 iterations, and identified 55 Pareto optimal parameters. For example, $\mathbf{x}_3$ in Fig. 5 corresponds to the parameter values $\mu = 28$ and $\xi = 0.58$, and it leads to $N_{\mathrm{Inc}} = 0.0003$ and $\mathrm{MCTR} = 1228$. This is a dominated solution because if we choose parameter values $\mu = 0$ and $\xi = 0.26$ ($\mathbf{x}_4$), then N_{Inc} is reduced to 0.0002 and MCTR is increased to 1233. In other words, we can improve both objectives. Thus, $\mathbf{x}_4$ is a Pareto optimal solution, while $\mathbf{x}_3$ is not.

The Pareto front in Fig. 5 shows a trade-off between reliability ($f2 : N_{\mathrm{Inc}}$) and cost-efficiency ($f_1 : \mathrm{MCTR}$). To increase the reliability of maintenance by reducing N_{Inc}, there must be a reduction in MCTR or a decrease of cost-effectiveness. The choice among the Pareto optimal solutions depends on the preference of decision makers. For instance, if the expected number of incidents is preferred to be below 0.05, then an optimal choice of parameters are $\mu = 23$ and $\xi = 0.84$ ($\mathbf{x}_5$ in Fig.5). This choice of design parameters lead to $N_{\mathrm{Inc}} = 0.046$ and $\mathrm{MCTR} = 1254$. Since $\mathbf{x}_5$ is a Pareto optimal solution, there is no other solution

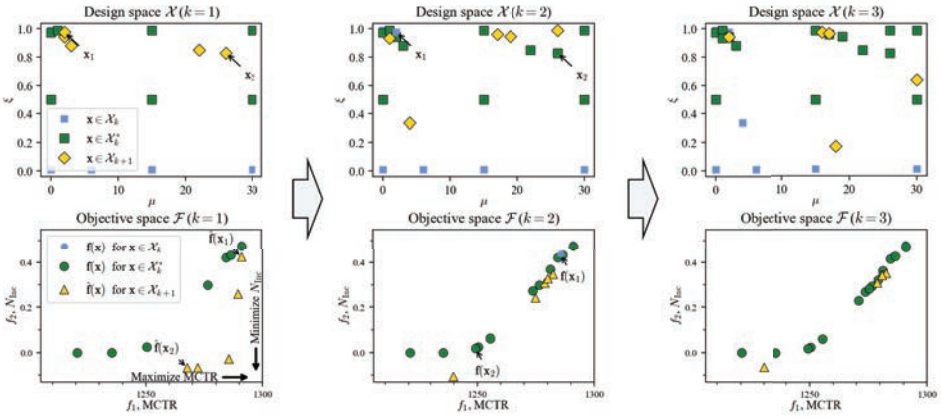

Fig. 4. Pareto optimal parameter values in objective space $\mathcal{F}$ and design space $\mathcal{D}$ during iterations $k = 1, 2, 3$.

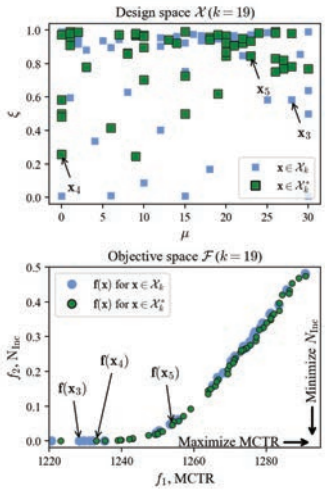

Fig. 5. Final result for the design of brake maintenance. (Up) The Pareto optimal parameters in the design space. (Down) The Pareto front in the objective space.

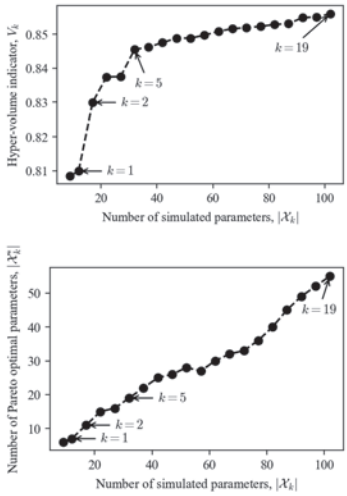

Fig. 6. Quality indicators at iteration k with respect to the number of simulated parameters.

that leads to a higher MCTR while maintaining $N_{\text{Inc}} \leq 0.5$.

4.2. *Quality of the Pareto front*

The quality of the Pareto front obtained by our approach is evaluated based on two indicators: the hyper-volume indicator V_k of the Pareto front, and the number of Pareto optimal parameters $|\mathcal{X}_k^*|$. V_k shows the level of exploration, while $|\mathcal{X}_k^*|$ shows the level of exploitation. Lee and Mitici (2022) Fig. 6 shows these quality indicators at iteration k, where its x-axes are the number of simulated parameters $|\mathcal{X}_k|$ representing the computational cost used until iteration k.

Based on Fig.6, we concluded that the identified Pareto front is satisfactory since the improvement of V_k (exploration) was slowed down. On the other hand, the number of Pareto optimal parameters $|\mathcal{X}_k^*|$ (exploitation) still increased significantly until the last iteration. This improvement of $|\mathcal{X}_k^*|$ was achieved by finding the Pareto optimal parameters that lead to very similar objective vectors $\mathbf{f}(\mathbf{x})$. This is clear in the final Pareto front

of Fig. 5, where many Pareto optimal objective vectors are similar.

The different trends of V_k and $|\mathcal{X}_k^*|$ in Fig. 6 show that our approach balances exploration and exploitation automatically. Large improvements of V_k during early iterations show that we first focused on exploration. For example, 78% of total improvements were made in $k \leq 5$. In the later iterations, however, we focused on the exploitation of the design space to identify more Pareto optimal parameters. Such a balancing is achieved by the utilization of both the GP models and our adaptive sampling approach.

5. Conclusion

In this study, we have proposed a methodology to design a reliable, data-driven maintenance for multi-component aircraft systems. We have considered a Gamma process for the degradation of system components, and ${}_N\mathrm{C}_M$ redundancy of such systems. The main contributions of this paper are:

- We propose Remaining-Useful-Life (RUL) prognostics using a Bayesian linear regression.
- We propose a data-driven maintenance strategy having two design parameters: a safety margin used in maintenance scheduling and a reliability threshold used to obtain RUL prognostics.
- We propose an algorithm to efficiently explore the design space of the safety margin and the reliability threshold, using Gaussian process learning and novel adaptive sampling techniques.
- We identify Pareto optimal, data-driven maintenance designs for aircraft landing gear systems, showing the trade-off between reliability and cost-efficiency objectives.

Overall, this study supports a transition towards the data-driven maintenance for aircraft systems by providing an efficient and reliable design framework.

Acknowledgement

This research has received funding from the European Union's Horizon 2020 research and innovation programme under grant agreement No 769288.

References

Arismendi, R., A. Barros, and J. Vatn (2019). Prognostics and Maintenance Optimization in Bridge Management Renny. *Proceedings of the 29th European Safety and Reliability Conference*, 978–981.

Chen, J., B. Xin, Z. Peng, L. Dou, and J. Zhang (2009). Optimal contraction theorem for exploration-exploitation tradeoff in search and optimization. *IEEE Transactions on Systems, Man, and Cybernetics Part A:Systems and Humans 39*(3), 680–691.

de Pater, I. and M. Mitici (2021). Predictive maintenance for multi-component systems of repairables with Remaining-Useful-Life prognostics and a limited stock of spare components. *Reliability Engineering and System Safety 214*, 107761.

de Pater, I., A. Reijns, and M. Mitici (2022). Alarm-based predictive maintenance scheduling for aircraft engines with imperfect Remaining Useful Life prognostics. *Reliability Engineering & System Safety 221*, 108341.

Kleijnen, J. P. (2008). Design Of Experiments: Overview. In *Proceedings of the 2008 Winter Simulation Conference*, pp. 479–488. IEEE.

Lee, J. and M. Mitici (2020). An integrated assessment of safety and efficiency of aircraft maintenance strategies using agent-based modelling and stochastic Petri nets. *Reliability Engineering and System Safety 202*, 107052.

Lee, J. and M. Mitici (2021). Multi-objective analysis of condition-based aircraft maintenance strategies using discrete event simulation. *Reliability and Maintainability Symposium*, 1–6.

Lee, J. and M. Mitici (2022). Multi-objective design of aircraft maintenance using Gaussian process learning and adaptive sampling. *Reliability Engineering and System Safety 218*, 108123.

Oikonomou, A., N. Eleftheroglou, F. Freeman, T. Loutas, and D. Zarouchas (2022). Remaining Useful Life Prognosis of Aircraft Brakes. *International Journal of Prognostics and Health Management 13*(1), 1–11.

Rasmussen, C. E. and C. K. I. Williams (2006). *Gaussian processes for machine learning*. MIT Press.

Rojas-Gonzalez, S. and I. Van Nieuwenhuyse (2020). A survey on kriging-based infill algorithms for multiobjective simulation optimization. *Computers and Operations Research 116*, 104869.

Zitzler, E., L. Thiele, M. Laumanns, C. M. Fonseca, and V. G. Da Fonseca (2003). Performance assessment of multiobjective optimizers: An analysis and review. *IEEE Transactions on Evolutionary Computation 7*(2), 117–132.